In tight junctions, claudins regulate the interactions between occludin, tricellulin and marvelD3, which, inversely, modulate claudin oligomerization

Jimmi Cording[1], Johanna Berg[1], Nadja Käding[1], Christian Bellmann[1], Christian Tscheik[1], Julie K. Westphal[2], Susanne Milatz[3], Dorothee Günzel[3], Hartwig Wolburg[4], Jörg Piontek[1], Otmar Huber[2] and Ingolf Ernst Blasig[1,*]

[1]Leibniz-Institut für Molekulare Pharmakologie, Robert-Rössle-Str. 10, 13125 Berlin, Germany
[2]Institute of Biochemistry II, Jena University Hospital, Nonnenplan 2, 07743 Jena, Germany
[3]Institut für Klinische Physiologie CBF, Charité, Freie Universität und Humboldt-Universität, Berlin
[4]Institute of Pathology and Neuropathology, Department of General Pathology, University of Tübingen, Medical School Tübingen, 72076 Germany
*Author for correspondence (iblasig@fmp-berlin.de)

Accepted 25 October 2012
Journal of Cell Science 126, 554–564

doi: 10.1242/jcs.114306

Summary

Tight junctions seal the paracellular cleft of epithelia and endothelia, form vital barriers between tissue compartments and consist of tight-junction-associated marvel proteins (TAMPs) and claudins. The function of TAMPs and the interaction with claudins are not understood. We therefore investigated the binding between the TAMPs occludin, tricellulin, and marvelD3 and their interaction with claudins in living tight-junction-free human embryonic kidney-293 cells. In contrast to claudins and occludin, tricellulin and marvelD3 showed no enrichment at cell–cell contacts indicating lack of homophilic *trans*-interaction between two opposing cell membranes. However, occludin, marvelD3 and tricellulin exhibited homophilic *cis*-interactions, along one plasma membrane, as measured by fluorescence resonance energy transfer. MarvelD3 also *cis*-interacted with occludin and tricellulin heterophilically. Classic claudins, such as claudin-1 to -5 may show *cis*-oligomerization with TAMPs, whereas the non-classic claudin-11 did not. Claudin-1 and -5 improved enrichment of occludin and tricellulin at cell–cell contacts. The low mobile claudin-1 reduced the membrane mobility of the highly mobile occludin and tricellulin, as studied by fluorescence recovery after photobleaching. Co-transfection of claudin-1 with TAMPs led to changes of the tight junction strand network of this claudin to a more physiological morphology, depicted by freeze-fracture electron microscopy. The results demonstrate multilateral interactions between the tight junction proteins, in which claudins determine the function of TAMPs and vice versa, and provide deeper insights into the tight junction assembly.

Key words: Claudins, Occludin, Tricellulin, MarvelD3, Tight junction, Protein interaction

Introduction

Tight junctions (TJs) seal the paracellular cleft of epithelial and endothelial cells most apical of the lateral cell membranes. They separate the internal space of multicellular organisms from external compartments, and form a paracellular diffusion barrier (Angelow et al., 2008). Ultrastructural analyses by freeze-fracture electron microscopy identify the TJs as a set of branched intramembranous strands of protein particles bringing the plasma membranes of opposing cells into molecular contact.

Occludin (Occl), marvelD3 (Md3) and claudin (Cld) proteins represent the major integral components of bicellular TJs (Furuse et al., 1998; Furuse et al., 1993; Raleigh et al., 2010; Steed et al., 2009). Tricellulin (Tric) is also characterized as an integral TJ protein, which predominantly localizes at tricellular TJs (Ikenouchi et al., 2005). All TJ proteins mentioned above contain four transmembrane domains with N- and C-terminal cytoplasmic tails, two extracelluar loops and a short intracellular loop. Occl, Tric and Md3 constitute the TJ-associated marvel protein (TAMP) family, based on their sequence homology within the shared marvel domain (MAL and related proteins for vesicle trafficking and membrane link) (Raleigh et al., 2010). The three-dimensional structures of Clds and TAMPs are unknown.

Occl has been identified as the first integral TJ protein (Furuse et al., 1993), nevertheless its functional role remains unclear. Although Occl is a specific component of all TJs, its knockout in mice does not show a phenotype with respect to TJ formation, strand morphology or barrier function (Saitou et al., 2000; Schulzke et al., 2005). Its C-terminus contains a coiled coil domain which is involved in a redox-sensitive dimerization of Occl (Walter et al., 2009) and in the association of *zonula occludens* protein 1 (ZO-1) (Müller et al., 2005). Occl is phosphorylated by different protein kinases on serine, threonine and tyrosine residues (for a review, see Dörfel and Huber, 2012). Typical kinases are conventional Ca^{2+} dependent and novel diacylglycerol dependent kinases (Andreeva et al., 2006), CK1, CK2 (Dörfel et al., 2009), c-Src (Kale et al., 2003), c-Yes (Chen et al., 2002) and activated, phosphorylated ERK_1 (extracellular signal related kinase) (Basuroy et al., 2006). Marchiando et al. found that Occl is involved in the maintenance of the barrier function *in vivo* (Marchiando et al., 2010). Occl derived peptides may disrupt TJ formation (reviewed by Blasig et al., 2011). Furthermore, it is suggested that Occl is *trans*-interacting via its extracellular loops (for review see Blasig et al., 2011).

Tric is preferentially localized at tricellular cell–cell contacts where the TJ network is extended basolaterally (Ikenouchi et al., 2005). After overexpression, Tric is also strongly detectable at bicellular contacts (Krug et al., 2009). Tric reveals extended N- and C-terminal cytoplasmic domains, with the C-terminal tail exhibiting homology to the Occl C-terminus (Ikenouchi et al., 2005). It has been shown that the C-terminus is important for the basolateral translocation of Tric (Westphal et al., 2010) and its binding to the lipolysis-stimulated lipoprotein receptor (LSR). LSR builds a landmark for tricellular TJs (Masuda et al., 2011). The N-terminal domain appears to be involved in directing Tric to tricellular contacts. Despite this homology, Occl and Tric are differentially phosphorylated in their C-terminal tails (Dörfel et al., 2009). Tric severely influences TJ organization not only at tricellular contacts but also at the level of bicellular TJs. The knockdown of Tric results in redistribution of Occl at bicellular TJs, i.e. tear-drop shaped accumulation of Occl close to tricellular TJs. Therefore, it is assumed that Tric and Occl may at least partially compensate each other (Ikenouchi et al., 2008). Mutations in the cytoplasmic C-terminal domain of Tric cause deafness (Riazuddin et al., 2006).

Md3 has recently been discovered as the latest TAMP member (Raleigh et al., 2010; Steed et al., 2009). It has an extended N-terminal and a short C-terminal tail, and is localized mainly at bicellular TJs. Knockdown results suggest retardation in junction formation (Raleigh et al., 2010). However, little is known about its molecular function.

Currently, 27 members of the Cld protein family have been identified in mammals (Mineta et al., 2011). While Clds share the tetraspan transmembrane topology with the TAMPs both families do not show considerable sequence homology. In addition, Clds are characterized by much shorter N- and C-terminal cytoplasmic domains compared to TAMPs. Clds can be subdivided in a highly homologous group of classic Clds including Cld1–10, 14, 15, 17 and 19, and the less homologous group of non-classic Cld11–13, 16, 18 and 20–27. Tissue-specific expression of different combinations of Clds defines the tissue-specific barrier characteristics (Krause et al., 2008). In this respect, expression of tightening Clds, such as Cld5 (Nitta et al., 2003; Piehl et al., 2010) has been demonstrated to seal the paracellular cleft. On the other hand, pore-forming Clds, such as Cld2 (Amasheh et al., 2002) facilitate paracellular ion permeability. The pore-forming function of a specific Cld is preferentially determined by the first extracellular loop (Amasheh et al., 2002) while the second extracellular loop rather supports tightening of the paracellular cleft (Piehl et al., 2010). Both homophilic and heterophilic *cis*- and *trans*-interactions have been observed between Clds (Basuroy et al., 2006; Furuse et al., 1999; Piontek et al., 2011).

The observations that TAMPs have overlapping properties and may partially replace each other (Raleigh et al., 2010) led us to the assumption that an interdependency between Tric, Occl and Md3 may be involved in the formation and organization of TJ strands. In consequence, this points to molecular interactions between the TAMPs in a homophilic and heterophilic manner. Taken together we hypothesize that associations between TAMPs as well as between TAMPs and Clds occur. Here, we present systematic live-cell evidence that TAMPs alone and Clds alone are able to oligomerize in a homophilic and heterophilic manner within their families, but also between members of both families. In conclusion, the data show that certain classic Clds influence the interaction between TAMPs. Conversely, the TAMPs also have the ability to modulate the oligomerization behavior of Clds.

Results

MarvelD3 colocalizes and interacts with tricellulin and occludin at cell–cell contacts but occludin does not interact with tricellulin

Similarly as described previously for Clds (Piontek et al., 2011), TJ-free human embryonic kidney (HEK)-293 cells were used to analyze the localization and ability of Occl, Tric and Md3 to form homophilic *trans*-interactions between two transfected cells (Fig. 1A). Occl was the only TAMP family member which showed enrichment at contacts between two Occl-expressing cells (contact enrichment). The enrichment factor of Occl (1.85 ± 0.31, $n=36$) was significantly different from that of the negative control corticotropin releasing factor receptor-1 (0.9 ± 0.05, $n=30$). For Tric (0.78 ± 0.19, $n=51$) and Md3 (1.0 ± 0.2, $n=31$), enrichment factors in the range of the negative control were observed (Fig. 1E). This indicates, that Occl is the only TAMP which is able to form homophilic *trans*-interactions.

Furthermore, we measured the fluorescence resonance energy transfer (FRET) as indicator of homophilic and heterophilic *cis*-interactions among members of the TAMP family along the cell membrane of one cell at cell–cell contacts (Fig. 1B–D,F). For every member of the TAMP family, the FRET efficiencies for the respective cyano fluorescence/yellow fluorescence protein (CFP/YFP) fusion pairs were significantly higher (Occl: $9.14\pm2.14\%$, $n=19$; Tric: $4.60\pm0.98\%$, $n=33$; Md3: $8.17\pm2.00\%$, $n=16$) than for the negative control Cld5/corticotropin releasing factor receptor-1 (0.92 ± 0.31, $n=9$). These data point to homophilic *cis*-interactions for all TAMPs. Heterophilic *cis*-interaction at cell–cell contacts could not be observed for Occl and Tric (FRET efficiency: $0.91\pm0.24\%$, $n=14$, both N-terminally tagged); also no *cis*-interaction was detected when Tric was C-terminally tagged with the fluorescent protein (CFP–Occl/Tric–YFP: $-2.84\pm1.40\%$, $n=5$). The results indicate that the two proteins do not physically interact with each other at bicellular contacts. By contrast, Md3 exhibits heterophilic interaction with both Occl and Tric (FRET efficiencies for Occl/Md3: $7.28\pm1.59\%$, $n=21$; Tric/Md3: $7.53\pm2.27\%$, $n=11$) as shown in Fig. 1F (values relative to the positive control Cld5–CFP/Cld5–YFP). In contrast, strong colocalization and FRET within intracellular compartments (YFP–Tric/CFP–Occl: FRET efficiency $3.81\pm0.75\%$) suggests an intracellular interaction between Occl and Tric in HEK cells probably during transport to the cell surface as discussed earlier (Westphal et al., 2010).

Coexpression of tricellulin or occludin but not marvelD3 with claudin-1 or -5 leads to enrichment of the TAMPs at cell contacts

We found an enrichment of Occl and Tric at cell–cell contacts when they were coexpressed with Cld1 or Cld5. The contact enrichment of Occl was significantly increased by the coexpression with Cld1 (enrichment factor: 2.54 ± 0.49, $n=27$) or Cld5 (2.57 ± 0.31, $n=36$) compared to the expression of Occl alone (1.85 ± 0.31, $n=36$) (Fig. 2A). In HEK-293 cells, Tric was located at bicellular contacts in contrast to the tricellular localization in epithelial cell lines endogenously expressing Tric (Westphal et al., 2010). When Tric was expressed alone in the HEK-293 cells no contact enrichment was detectable at

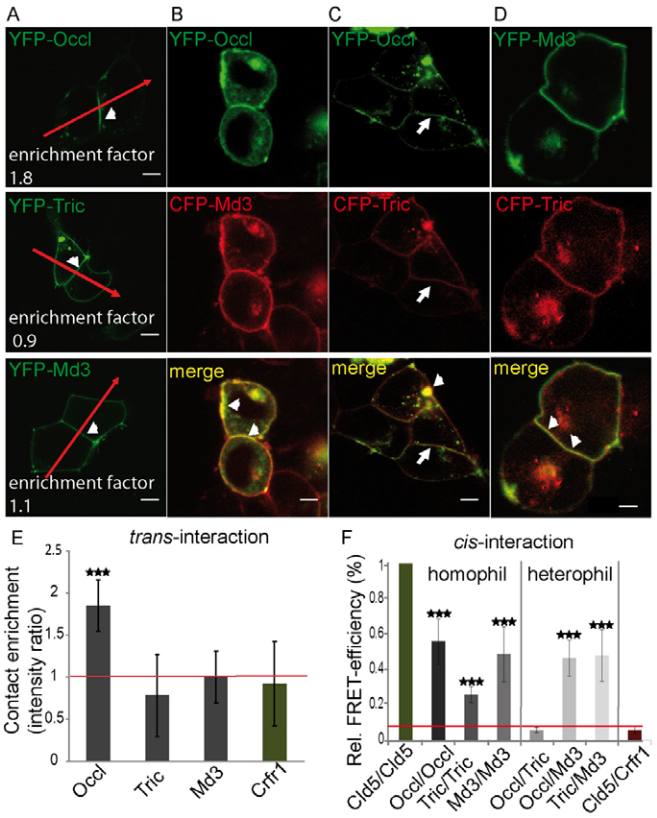

Fig. 1. Homophilic and heterophilic colocalization and interactions between TAMPs. (**A–D**) Live cell fluorescence imaging of HEK-293 cells transfected with members of the TAMP family; YFP–TAMP (green)/CFP–TAMP (red), colocalization (yellow). (A) YFP–Occl exhibits homophilic contact enrichment at cell–cell contacts between two transfected cells (arrowhead) compared to a contact between a transfected and non-transfected cell along the red arrow, whereas neither Tric nor Md3 do so (arrowheads). (B) Coexpression of YFP–Occl/CFP–Md3 leads to their colocalization at the plasma membrane (arrowheads). (C) For coexpression of YFP–Occl/CFP–Tric, colocalization (arrowhead) is detected intracellularly; both proteins are localized at the same cell–cell contact (arrow). (D) YFP–Md3/CFP–Tric shows colocalization at the plasma membrane (arrowheads). (**E**) Only, *trans*-interaction of YFP–Occl is detectable compared to the negative control Crfr1, quantified as fluorescence enrichment at the contacts between two transfected cells. (**F**) Homophilic and heterophilic *cis*-interactions between members of the TAMP family measured by FRET. All TAMPs show homophilic association; heterophilic binding is detected between Md3 and Tric as well as Md3 and Occl within cell–cell contacts but not between Occl and Tric. Co-transfected Cld5–YFP/Crfr1–CFP and Cld5–YFP/–CFP are used as negative (red column) and positive control (green column), respectively. FRET efficiencies relative to that of the positive control are depicted. For each construct, 9–33 different cell–cell contacts were analyzed. Values are means ± s.e.m.; ***$P<0.001$ compared to negative control. Scale bars: 5 µm. Red line separates enrichment and FRET values in the range of the negative control from those above them.

bicellular contacts (enrichment factor: 0.78±0.19, $n=51$). Interestingly, coexpression with Cld1 caused a strong contact enrichment of Tric at bicellular cell–cell contacts (6.38±1.11, $n=33$) whereas coexpression of Cld5 with Tric only resulted in a minor increase of the contact enrichment of Tric (1.60±0.21, $n=57$) considerably less but still significantly different compared to the monoexpressed Tric. Md3, when expressed alone, showed no enrichment at cell–cell contacts (1.0±0.2, $n=31$). In contrast to Occl and Tric, coexpression of Cld1 or Cld5 revealed no effect on the enrichment factor of Md3 (Cld1: 1.03±0.2, $n=27$; Cld5: 0.83±0.2, $n=18$; Fig. 2A). The values determined were not influenced by the amount of the proteins studied as western blots demonstrated similar expression levels of specific TAMPs in the different co-transfections (Fig. 2C). In addition, the enrichment found was not changed when the fluorescence proteins were replaced by a FLAG-tag (Fig. 2D).

TAMPs show a high heterophilic *cis*-interaction potential with claudin-1, marvelD3 additionally *cis*-interacts with claudin-3

To gain insight into interactions between Clds and TAMPs we analyzed the colocalization of TAMPs with selected Clds (supplementary material Fig. S1) as well as their association within one plasma membrane (*cis*-interaction) using FRET assay in HEK-293 cells (Fig. 2B). Cld1 exhibited a high potential to interact with Occl (FRET efficiency: 8.69±2.00%, $n=19$), with Tric (12.6±3.63%, $n=12$) and with Md3 (8.10±2.25%, $n=13$). Other classic Clds showed a weak interaction with TAMPs, except the pair Md3 and Cld3. For instance, Cld2 exhibited a significant interaction with Occl, FRET efficiency 3.70±1.32%, $n=9$, whereas no interaction with Tric (0±0%, $n=7$) and Md3 (1.43±0.38%, $n=14$) was detectable. Cld3 was interacting with Md3 (FRET efficiency: 8.23±1.68%, $n=24$) but not with Occl (2.49±0.79%, $n=10$) and only at a minor level with Tric (4.24±1.28%, $n=11$). Cld4 had a low interaction potential with all of the three TAMPs, which was still significantly different from the negative control: FRET efficiency with Occl 4.13±1.19% ($n=12$), with Tric 4.77±1.40% ($n=9$) and with Md3 5.00±1.02% ($n=24$). Cld5 exhibited a low, non-significant potential to oligomerize with Occl (1.77±0.44%, $n=16$), whereas the interaction potential with Tric (4.03±0.68, $n=22$) and with Md3 (4.32±1.25%, $n=16$) differed significantly from the negative control. The non-classic Cld11 was highly colocalizing with all TAMPs (supplementary material Fig. S1). However, no *cis*-interaction of Cld11 with any of the TAMPs was observed (Fig. 2B), although Cld11 was clearly capable of homophilic *cis*-interaction (FRET efficiency 24.58±1.62%, $n=14$) as well as of homophilic *trans*-interaction (enrichment factor 18.4±2.77, $n=20$).

In the cell–cell contacts of Madin-Darby canine kidney (MDCK-II) cells forming TJ endogenously, significantly higher FRET values were determined compared to the negative control (Cld1–YFP/corticotropin releasing factor receptor 1–CFP, −4.22±1.83%): Cld1–YFP/CFP–Occl, 4.66±2.25%; Cld1–YFP/CFP–Tric, 7.68±1.88%; Cld1–YFP/CFP–Md3, 3.50±02.37% ($n\geq9$, $P<0.05$).

When tricellulin and claudin-1 are expressed with occludin, tricellulin loses its enrichment at bicellular tight junctions and its colocalization with claudin-1

Tric, when expressed in TJ-free HEK-293 cells, was localized throughout the plasma membrane (Fig. 1A). However, when coexpressed with Cld1 it was enriched at bicellular contact sites (Fig. 2A; supplementary material Fig. S1, upper left). In TJ-forming cells, such as human colon carcinoma cells (Caco-2; Fig. 4C, third row) or MDCK-II (supplementary material Fig. S2, upper block), Tric was preferentially localized at tricellular contacts similar as found earlier (Ikenouchi et al., 2008). When we analyzed HEK-293 cells transfected with YFP-Occl,

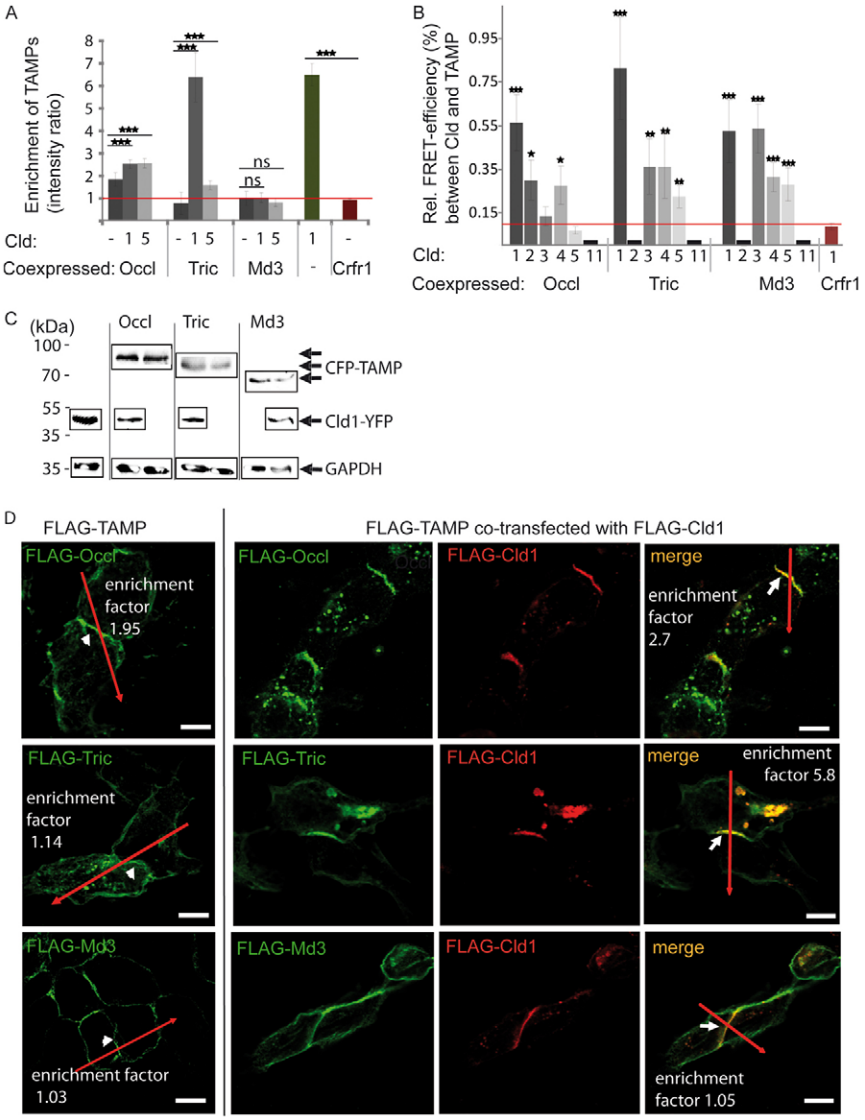

Fig. 2. Co-enrichment and fluorescence resonance energy transfer analyses indicate subtype-specific claudin–TAMP interactions. (**A**) Claudin-1 and -5 improve the enrichment of Occl and induce enrichment of Tric between two opposing cells, compared to the respective TAMP-control-transfected alone. Quantification of TAMP enrichment at cell–cell contacts between living HEK-293 cells transfected with a YFP–TAMP alone or together with either FLAG–claudin-1 or -5 was measured by transcellular fluorescence cell scanning. The plasma membrane was visualized with Trypan Blue. HEK-293 cells transfected with Cld1–YFP were used as positive control and the negative control was Crfr1–CFP. Values are means ± s.e.m.; ***$P<0.001$ compared as indicated by the black horizontal lines; ns, non-significant difference; $n\geq18$ in each group. (**B**) The classic claudins-1–5, but not the non-classic claudin-11 are able to *cis*-interact with the TAMPs to a different extent. HEK cells were co-transfected with Cld(1–5)–YFP and CFP–TAMP members. Co-transfection of Cld1–YFP and Crfr1–CFP was used as negative control. For FRET measurements with CFP–Cld11, YFP–TAMP constructs were used. Values are means ± s.e.m.; *$P<0.05$, *$P<0.01$ and ***$P<0.001$, respectively, compared to Crfr1–CFP/Cld1–YFP; $n=6$–30. The red lines separate values of the negative control from values above them. (**C**) Western blot analyses of HEK cells transfected with a CFP-TAMP alone or CFP-TAMP and Cld1-YFP show that the TAMP and the Cld are expressed to a similar extent and that the coexpression does not influence the expression level of the specific TAMPs. As a loading control GAPDH was used. (**D**) To confirm that the YFP and CFP tags used in A and B do not influence the properties (white arrows) of the TJ proteins, HEK cells were transfected with FLAG-tagged TAMPs and FLAG-tagged Cld1. Left column, FLAG–Occl exhibits homophilic contact enrichment at cell–cell contacts between two transfected cells (arrowhead) compared to a contact between a transfected and non-transfected cell along the red arrow, whereas neither FLAG–Tric nor FLAG–Md3 do so (arrowheads). Scale bars: 5 µm.

CFP-Tric and/or FLAG-Cld1 in respect to Tric enrichment at bicellular contact sites Occl was well enriched in the contact area between two transfected cells (enrichment factor 2.54±0.49, $n=13$), whereas Tric was present throughout the membrane but was not enriched at cell contacts any more (0.97±0.05, $n=14$; Fig. 3). This is in contrast to the coexpression of Cld1 and Tric, where Tric was enriched at bicellular contact sites (6.38±1.11, $n=33$).

The co-expression of claudin-1 defines occludin and tricellulin mobility and distribution at bicellular contacts

Based on the detected interactions and changes in the subcellular localization of TAMPs after co-transfection with Cld1, we measured the mobility of TAMPs in the plasma membrane of HEK-293 cells at cell–cell contact sites, when expressed alone and together with FLAG–Cld1. Cld1 itself showed low mobility at cell–cell contacts (mobile fraction 16.2±4.6%, $n=6$; Fig. 4A,B), due to the strong *trans*-interaction of the protein (see Fig. 2A). Occl was highly mobile when expressed alone (57.4±3.9%, $n=6$). Similar differences were found in MDCK-II cells, ~40% mobile fraction for Cld1 and ~70% for Occl (Shen et al., 2008). When coexpressed with FLAG–Cld1, the mobility of Occl was reduced (mobile fraction 25.8±6.7%, $n=6$). Tric alone was also highly mobile at areas of cell–cell contacts (mobile fraction 74.4±4.45%, $n=7$) and the mobility was strongly reduced after coexpression of FLAG–Cld1 (17.7±7.3%, $n=8$). In contrast, there were no significant effects on the mobility of Md3 (55.5±4.1%, $n=7$) after coexpression of Cld1 (50.2±8.1%, $n=6$; Fig. 4B). These findings were supported by the Cld1 knockdown experiments in Caco-2 cells. The knockdown of Cld1 led to a redistribution of Tric from tricellular contact sites to stretches of bicellular contacts (Fig. 4C). The plasma membrane localization of Cld1 was lost after treatment with the siRNA, whereas other TJ proteins like ZO-1 (Fig. 4C) or Cld2 (data not shown) were not affected. The effect on Tric caused by the knockdown of Cld1 in the Caco-2 cells was not influenced by the amount of the proteins as western blot analysis demonstrated similar expression levels of Tric after Cld1 knockdown compared to the control (Fig. 4D).

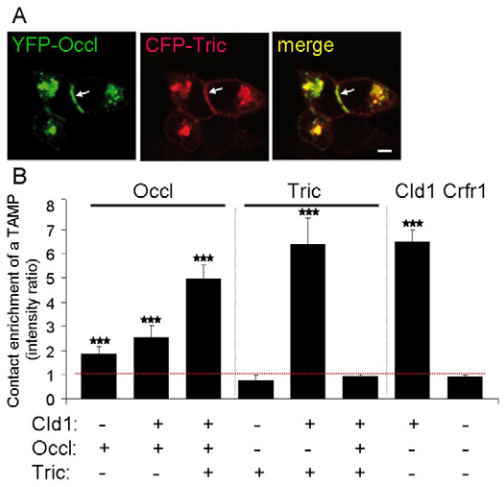

Fig. 3. Occludin displaces tricellulin from claudin-1. In the absence of Occl, Tric is co-enriched at bicellular cell–cell contacts with Cld1 in living HEK-293 cells. (**A**) The co-enrichment of CFP–Tric with Cld1 in bicellular contacts is abolished if CFP–Tric is triple-transfected with YFP–Occl and FLAG–Cld1, as shown by fluorescence images showing cell–cell contact enrichment of Occl but not of Tric (arrows). Furthermore, membrane localization of Tric at cell–cell contacts is reduced. (**B**) Quantification of the bicellular contact enrichment of YFP–Occl or YFP–Tric expressed alone, coexpressed with FLAG–Cld1 or tri-expressed (CFP–Tric, FLAG–Cld1, YFP–Occl; YFP–Tric, FLAG–Cld1, CFP–Occl) shows enrichment of Occl or Tric after coexpression of the TAMP and Cld1. Tric, however, is completely prevented from localizing at the bicellular contact by the presence of Occl and Cld1. Scale bar: 5 μm; values are means ± s.e.m.; ***$P<0.001$ compared to the negative control, Crfr1; $n=13$. The dotted red line separates contact enrichment values of the negative control from values above them. Cld1 was used as positive control.

TAMPs modulate the tight junction strand morphology of claudin-1

Finally, we investigated the morphology of TJ strands in HEK-293 cells transfected with Cld1 alone or together with Occl, Tric or Md3, by freeze-fracture electron microscopy (Fig. 5). Fig. 5A–F depict the TJ strand network and Fig. 5G the quantification of mesh size and parallel strands. The most obvious observation through all experiments was the high, almost complete association of the TJ strands with the protoplasmic fracture face and their continuous appearance. Cld1 transfected HEK-293 cells revealed an extended meshwork of TJ strands in the range of 15 meshes/μm^2 (Fig. 5A). Rarely, the TJ strands were closely arranged in a parallel fashion without or with few branch points of the network (as in Fig. 5D; around 10% of the total TJ strand area). Co-transfection of Cld1 and Tric changed the TJ network from round-shaped strands to more rectangular meshes with reduced mesh size (about 54 meshes/μm^2) and a negligible small number of parallel strands, but maintained high protoplasmic fracture face association (Fig. 5B). Interestingly, the TJs occasionally formed discontinuous insulated strand arrangements which were associated with small gap junctions (data not shown). Cld1/Md3 co-transfected HEK-293 cells revealed TJs which resembled the TJ network of cells transfected with Cld1 alone (Fig. 5A); however, the meshes were smaller (32 meshes/μm^2; Fig. 5C). In addition, in places we found large membrane areas with lots of parallel strands without any bifurcation (Fig. 5D; about 24% of the total TJ strand area). However, as mentioned above, this spectacular arrangement can also be formed with Cld1 alone, but substantially less frequent. The Cld1/Occl co-transfected cells predominantly showed similar elongated TJ networks as the Cld1 mono-transfected cells, but frequently short pieces of bundled TJ strands were observed (Fig. 5E; about 26% parallel area of the total TJ strand area). Perhaps more importantly, many strands associated with the protoplasmic fracture face were interrupted without an increase of particles at the exoplasmic fracture face (Fig. 5F). These discontinuities reflect a loss of particles from the Cld1-based TJ strands obviously induced by the co-transfection with Occl. Tric alone formed short, discontinuous up to continuous and seldom branched strands on the protoplasmic fracture face (supplementary material Fig. S3) whereas mono-transfected Occl or Md3 did not in the HEK-293 cells used.

Discussion

We here report systematic cell biological studies elucidating the ability of TAMPs to form homophilic and heterophilic complexes within this family as well as heterophilic complexes with members of the Cld family. These studies demonstrate that in TJ strands a multitude of different heterophilic interactions of classic Clds and of the TAMPs determine TJ assembly and structure. On the other hand, TAMPs may modulate the oligomerization behavior of Clds.

For the first time, we performed a quantitative analysis of the oligomerization potential within the TAMP family, showing the most pronounced *trans*- and *cis*-interaction between Occl molecules. This verifies and expands the knowledge gained by co-immunoprecipitation (Blasig et al., 2006; Raleigh et al., 2011), a procedure which does not allow an explicit differentiation between *trans*- and *cis*-interactions. In contrast, Tric and Md3 do not show homophilic *trans*-interaction, whereas all TAMPs can form homophilic *cis*-interactions (FRET values Occl>Md3>Tric). Compared to homophilic Cld associations such as Cld1–Cld1 or Cld5–Cld5, the TAMP–TAMP interactions are less efficient.

Due to the homology of the marvel domain of the TAMPs and the great variation in the length of their cytosolic tails a heterophilic interaction between the transmembrane domains of all three members has been assumed (Blasig et al., 2011; Westphal et al., 2010). As a matter of fact, Md3 is interacting with both Occl and Tric, at bicellular cell–cell contacts within one plasma membrane (*cis*-interaction). However, interactions between the homologous marvel domains is unlikely as Occl and Tric are unable to associate heterophilically in the cell contact. Occl and Tric share a homologous coiled-coil and ELL-domain, respectively, which is absent in Md3 (Blasig et al., 2011). Md3 has only an extended N-terminal tail and nearly no C-terminal tail in the cytosol as an intracellular interaction site for cytosolic *cis*-binding domains of Occl and Tric.

However, we could not detect any heterophilic oligomerization within one plasma membrane between Occl and Tric, similarly as reported (Raleigh et al., 2010). This report detected no interactions between Occl and Tric by co-immunoprecipitation using Caco-2 cell lysates. On the other hand, they also found complexes between Md3 and Occl or Tric. In another study, it was shown with transfected HEK-293 cell lysates by co-immunoprecipitation (Westphal et al., 2010) that Occl and Tric physically form a complex. Experiments with deletion mutants of Tric used in the latter study suggested that this interaction may

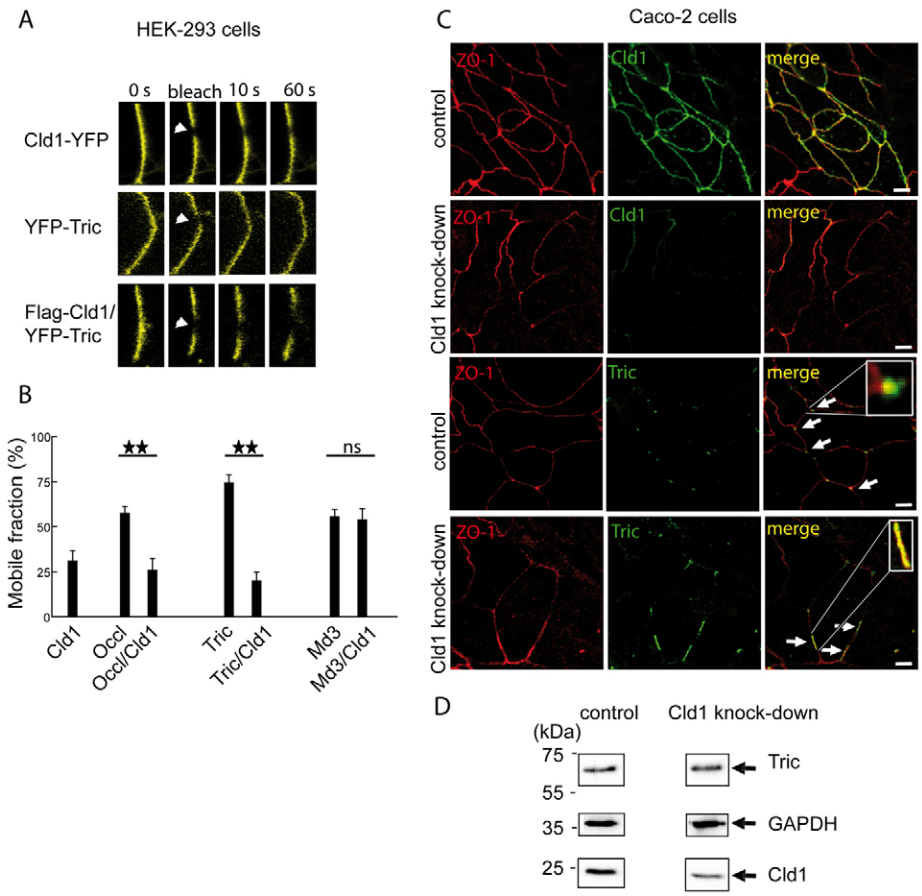

Fig. 4. The membrane mobility of tricellulin and occludin is highly reduced after coexpression of claudin-1. (**A**,**B**) HEK-293 cells were transfected with either Cld1-YFP, YFP-TAMP or co-transfected with FLAG-Cld1/YFP-TAMP. YFP within a particular area of the cell–cell contact was bleached and the time required for recovery of its fluorescence was determined in this area by FRAP for calculation of the mobile fraction in the plasma membrane of a cell contact. Examples of time series for the recovery of the YFP signal of Cld1 and Tric as well as of FLAG–Cld1/YFP–Tric before, during (arrowhead) and after bleaching are shown. (B) Mobile fractions of YFP-TAMPs transfected alone are considerably higher than that of Cld1–YFP alone. The mobility of Occl and Tric but not that of Md3 were clearly reduced after co-transfection with FLAG-Cld1. Values are means ± s.e.m., $n=10$; $^{**}P<0.01$; ns, not significant; comparison indicated by black lines. (**C**) Co-immunofluorescence staining of Cld1 or Tric (green) and ZO-1 (red) in Caco-2 cells 48 h after transfection with siRNA targeting Cld1 (second and fourth row) and of control-transfected wild-type cells (first and third row; scrambled Cld1 siRNA). After knockdown of Cld1 (second row), the Tric signal redistributes from tricellular to bicellular TJ (arrows; last row). Scale bars: 10 µm. (**D**) Western blot analyses of Caco-2 cells transfected with siRNA targeting Cld1 (Cld1 knockdown) in comparison to the control-transfected cells show that the expression level of Tric was similar and, hence, not affected by the Cld1 knockdown. GAPDH was the loading control.

occur during the transport of Occl and Tric to the cell membrane. Now, we can show by means of FRET that these complexes occur only in intracellular compartments, but not in the plasma membrane of co-transfected HEK-293 cells. In respect to the interplay of Occl and Tric, our results taken together with literature data (Ikenouchi et al., 2008; Raleigh et al., 2010) support the assumption that Occl and Tric may displace each other at cellular contacts. Owing to the different distribution in the plasma membrane of epithelial cells and also the weak membranous colocalization in HEK-293 cells, a direct interaction at cell–cell contacts appears unlikely.

In this work, we provide evidence for a strong interaction/oligomerization of members of the TAMP family with some of the investigated Clds. We verified this interplay by colocalization studies, FRET- and *trans*-interaction assays. The methods were successfully established to investigate Cld–Cld-interactions (Piontek et al., 2008). Interactions between the TAMPs and Clds have been postulated based on colocalization in L-fibroblasts (Raleigh et al., 2010) and co-precipitation in Caco-2 lysates with fragments of Occl (Raleigh et al., 2011). However, the exact binding properties have not been analyzed in the living cell so far. Cld1 exhibits a strong FRET signal with every TAMP member. Thus, this interaction should be of general importance in epithelial tissues. Cld3 also reveals a strong FRET signal with Md3, and a weaker signal with Tric, but none with Occl. Interactions with the Clds 2, 4 and 5 are considerably weaker. The ranking of the FRET values is Cld1>Cld4=Cld2 for Occl, Cld1>Cld4=Cld3=Cld5 for Tric, and Cld1=Cld3>Cld4=Cld5 for Md3. Also co-precipitation with recombinant GST fusion proteins of the cytosolic C-terminal tail of Occl in cell lysates captured Cld1, and to half amount, Cld2 (Raleigh et al., 2011), i.e. in the same ratio as determined in our FRET assays. From this observation, we assume a role of the C-terminal coiled coil domain (Walter et al., 2009) in the *cis*-interaction of a suitable

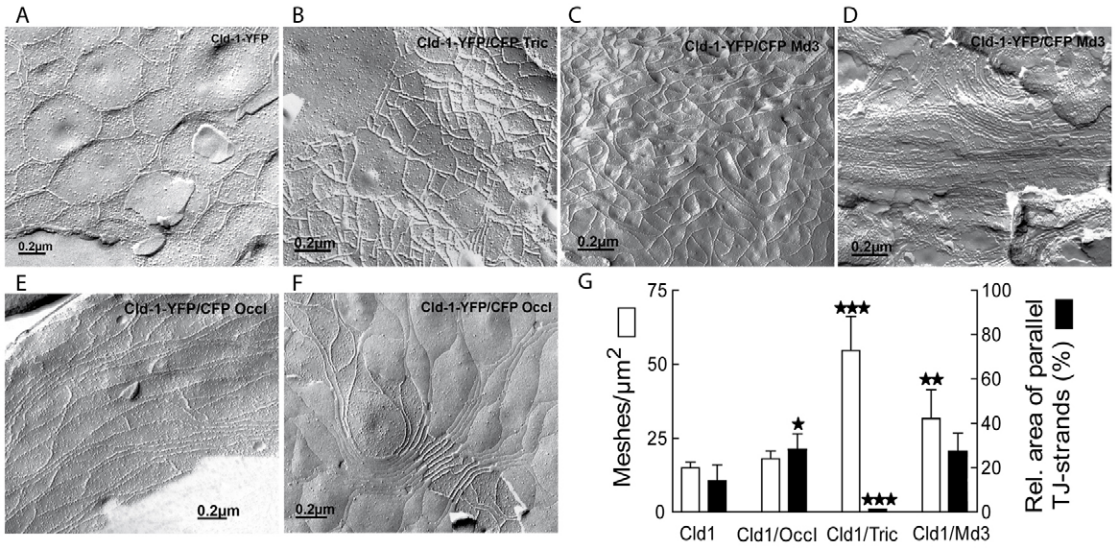

Fig. 5. TAMPs modulate the morphology of claudin-1 tight junction strands. Tric and Md3 co-transfected with Cld1 change the rounded strand network of the Cld to rectangular meshes and reduce the mesh size, whereas coexpression of Occl leads to elongated meshes. Transiently transfected HEK-293 cells where analyzed by freeze-fracture electron microscopy. (**A**) Cld1–YFP transfected alone, (**B**) co-transfected with CFP-Tric, (**C**,**D**) co-transfected with CFP-Md3, (**E**,**F**) co-transfected with Occl. (**G**) Quantification of the number of meshes per µm^2 (white columns) as well as the area of parallel strands in the total strand area (black columns; %), formed by Cld1 alone and after coexpression with the different TAMPs. Values are means ± s.e.m.; *P<0.05, **P<0.01 and ***P<0.001, respectively, compared to the corresponding mono-transfected Cld1 control; ≥10 independent images analyzed. For a further description, see text. Scale bars: 0.2 µm.

Cld with Occl. The non-classic Cld11 has not interacted with the TAMPs, reflected by a FRET-signal in the range of the negative control. Interactions between Occl and Clds are indicated by a previous FRET assay (Harris et al., 2010). However, Harris and co-workers calculated the percentage of FRET-positive pixels resulting in relative values. In contrast, we were able to detect absolute values by measuring the direct increase in the donor emission. Due to the different procedures the values cannot be compared. In conclusion, Cld1 shows a striking colocalization and interaction with the TAMP-family members at cell–cell contacts. Similar colocalization has been observed for Cld1 with Tric (Ikenouchi et al., 2008) and with TAMPs (Raleigh et al., 2010), but both groups have not demonstrated a direct association of the proteins. Cld1 is expressed in a multitude of tissues, similar to the TAMPs. This leads to the assumption that the interplay with Cld1 is of general relevance as an organizing protein for the assembly of the TAMPs in the TJs.

In our study, we have analyzed Clds and TAMPs in living cells allowing the investigation of interactions under physiological conditions. It has to be considered that the assays used do not directly measure the physical association between two proteins. They trace the interactions by indirect parameters such as contact enrichment, TJ-strand formation and FRET. However in cases where we obtained efficient FRET signals, the distance between the CFP and YFP tags used for the assay is less than 7 nm (Sekar and Periasamy, 2003). Hence, the FRET signals demonstrate a spatial proximity between the tested protein pair within one membrane at a cell–cell contact, which is within the distance known for a direct protein-protein binding. Thus, we can assume that the FRET signal is promoted by direct *cis*-interactions.

The interaction sites between Clds and TAMPs cannot be identified by our study. Raleigh et al. discussed that ZO-1 is the intermediate in Occl interactions with Cld1 and -2 (Raleigh et al., 2011). The cytosolic C-terminal coiled coil domain of Occl is known to attract the SH3-hinge-GuK unit of ZO-1 (Bal et al., 2012). And PDZ domains of ZO proteins bind to the C-termini of Clds (Itoh et al., 1999). Consequently, ZO proteins would bring together the Clds and Occl. We also see *cis*-associations between the latter two proteins. However, an interplay with ZO-1 can be excluded as, in our approach, the C-termini of the Clds are covered by fluorescent fusion proteins and, hence, are not accessible for PDZ domains. As the TAMPs are N-terminally fused with the fluorescence proteins an interaction of their N-terminal parts with the C-terminal Cld parts might be possible. In this case, the fluorescence proteins would come into an optimal distance for the FRET assay used to measure the *cis*-interaction.

Furthermore, we report a striking modification of the intercellular interaction properties of Occl and, especially, of Tric due to the coexpression with Cld1 or Cld5. When Tric is expressed alone in HEK-293 cells it is unable to interact homophilically in *trans*-between two neighboring cells as indicated by no enrichment of the protein. The coexpression of Occl or Tric with one of the mentioned Clds leads to increased co-enrichment of the respective TAMP at cell–cell contacts, supporting the assumption of an improved homophilic *trans*-interaction of Occl. Alternatively, it cannot be excluded that the apparently improved *trans*-interaction of Occl is indirectly caused by the *cis*- and *trans*-interaction of Cld1. For Tric, only a heterophilic association with a Cld should have caused the enrichment of Tric at the cell contact since homophilic *trans*-interaction was not detectable for Tric alone. This influence further underlines the existence of a direct association of Clds with the two TAMPs, which in consequence recruits more TAMP molecules to the cell–cell contacts resulting in enhanced co-

enrichment. The conclusion is supported by the FRAP measurements showing a drastic reduction of the membrane mobility of both Occl and especially of Tric in the presence of Cld1. An effect for Cld1 on TAMPs was reported earlier (Furuse et al., 1998; Ikenouchi et al., 2008; Raleigh et al., 2010) showing a strong redistribution of a TAMP from the periphery of the cell membrane to cell–cell contacts due to the coexpression with Cld1 in L-fibroblasts. To elucidate an influence of TAMPs on the Cld1-based TJ network we performed freeze-fracture electron microscopic analyses after co-transfection with Occl, Tric or Md3. Earlier, it has been demonstrated that Occl forms a small number of short TJ strand-like structures in L-fibroblasts (Furuse et al., 1993). For Tric (Ikenouchi et al., 2005) and Md3 (Raleigh et al., 2010), it was proposed, that they are unable to form TJ-like structures on their own. We here demonstrate that Tric is able to build a small number of short TJ strand-like structures similar as reported by Furuse et al. (Furuse et al., 1993) for Occl in fibroblasts. However, the Tric structures are negligible compared to those formed by Clds. Furthermore, we were not able to find such structures for Occl and Md3 in the HEK cells.

In freeze-fracture replicas of co-transfected HEK-293 cells (Occl/Cld1, Tric/Cld1 and Md3/Cld1), we demonstrate that these TAMPs specifically modify the TJ network of Cld1 exhibiting large round meshes rarely with parallel strands. Occl, caused more longitudinal meshes of Cld1, more parallel and less continuous strands. Tric reduces the mesh size four to five times and makes the shape strikingly rectangular which is comparable with other observations in size and shape (Ikenouchi et al., 2008). Md3 has a similar but less pronounced effect. In addition, it enhances the amount of parallel strands forming strand bundles and restricting network formation. In general, Tric, Md3 and to a lower extent Occl enable a more compact and integrated Cld1 strand morphology similar as occurring physiologically. Small and rectangular TJ strands are well known from epithelial cells expressing Clds and TAMPs endogenously (Piehl et al., 2010).

The Cld1–TAMP interactions seem to play an important role, especially, for the antagonistic behavior of Occl and Tric at bicellular contacts. Obviously, Clds (Piontek et al., 2011) and TAMPs, as shown in this study for Occl and Tric, are transported to the plasma membrane simultaneously as indicated by intracellular FRET measurements. This is also confirmed in our Ca^{2+}-switch experiment for Cld1 and Tric, which both reappear in the cell membrane at the same time (supplementary material Fig. S2). At bicellular contacts, Occl and Tric compete for the binding to Cld1, as we demonstrated in the triple-transfection experiment. Here, the interaction between Occl and Cld1 is stronger or more stable than Cld1/Tric, because Occl in addition to its binding to Cld1, is immobilized at the plasma membrane due to its relative strong homophilic *trans*-interactions. In contrast, Tric is unable to *trans*-interact homophilically. In addition, the Occl–Tric antagonism depends on Cld1 as suggested by the knockdown of Cld1 where Tric appears fragmented also in the bicellular contacts of Occl-expressing Caco-2 cells. In epithelial cells, the interaction of Cld1 and Tric does not occur at bicellular TJs (Raleigh et al., 2010). Taken together, our and literature data support the concept that Occl displaces Tric from bicellular to the tricellular TJs but only in the presence of a Cld such as Cld1. In the specialized tricellular structures, Tric is also captured by LSR a specific tricellular contact protein (Masuda et al., 2011) via the C-terminal tail of Tric. Owing to the interplay with Cld1, Occl (Ikenouchi et al., 2008) and LSR (Masuda et al., 2011), the tricellular localization of Tric is stabilized. In the tricellular cell contacts, Tric is interacting with Cld1 and organizes the proper tricellular TJ assembly. Md3 and Occl, which are localized at the bicellular TJs, are organizing the proper bicellular TJ assembly together with the Clds, since the two TAMPs localize together with Cld1 at bicellular TJs and modulate the structure of the strand network.

The interactions observed in non-TJ-forming HEK cells reflect physiologically relevant properties in cells that form TJs. Previously we reported *cis*-associations between Cld5–YFP and Cld5–CFP as well as YFP–Tric and CFP–Tric in TJ-forming MDCK-II cells (Westphal et al., 2010). Now, we demonstrate FRET for Cld1–YFP/CFP–Occl, Cld1–YFP/CFP–Tric, and Cld1–YFP/CFP–Md3 in the MDCK-II cells similar as in the HEK cells. The associations between the YFP- and/or CFP-fusion proteins presented here are neither affected by the fluorescent protein nor by the position of the tag. Earlier reports show homophilic co-immunoprecipitation for native Occl (Raleigh et al., 2010) or between C-terminally tagged Occl–His and Occl–FLAG (Blasig et al., 2006), which corresponds to our data with N-terminal fusion proteins: the enrichment of YFP–Occl in cell contacts and the *cis*-interaction for YFP– and CFP–Occl. In addition, N-terminal FLAG–Tric has failed to show enrichment in cell–cell contacts (Westphal et al., 2010), the same as we see with YFP–Tric. CFP–Tric and Tric–CFP, tagged N- and C-terminally, respectively, resulted in comparable FRET signals with YFP– and CFP–Tric (Westphal et al., 2010) similar as in co-precipitation of tag-free Tric (Raleigh et al., 2010). An Occl–Tric interaction cannot be visualized regardless of a N- or C-terminal position of the fluorescent protein. This is in agreement with pull-down experiments with tag-free Occl and Tric, which also do not co-precipitate (Raleigh et al., 2010). The binding between non-tagged Cld1 and a GST fusion protein of the cytosolic C-terminal tail of Occl detected by a pulldown (Raleigh et al., 2011) is specifically confirmed by our FRET measurements. Finally, we demonstrate that the FLAG–Cld1/FLAG–TAMP associations are not different from those between fluorescently tagged proteins. All these examples provide evidence that the tags of the Clds and TAMPs studied do not disturb their interplays.

As an independent approach to support that the associations observed by FRET in HEK cells are also relevant for TJs formed endogenously, a proximity ligation assay (PLA) was performed in MDCK-II cells (supplementary material Fig. S4). With PLA, the proximity of two proteins within 50 nm distance can be detected. Proximity at cell–cell contacts was clearly observed for Cld1/Occl but not for the Cld1/glyceraldehydes 3-phosphate dehydrogenase (GAPDH) control. This result suggests that the interactions detected by FRET in the HEK cells system are relevant for endogenous TJ proteins in fully polarized epithelial cells. However, the FRET assays in the HEK cells have the advantage of restricting the proximity-based signal to <7 nm, better quantification and excluding indirect interactions via additional TJ proteins.

Taken together, our results are consistent with following model for the TJ assembly in a barrier-forming cell. Occl$>$Md3$>$Tric (intensity order) compete for binding to the Cld oligomers, as shown by the contact enrichment, FRET or FRAP studies. Consequently, Occl and Md3 bind extensively to Cld1 at the bicellular contact, similar as Md3 to Cld3 (Table 1); in contrast, Tric is shifted to the tricellular corner. Due to these interactions

Table 1. Overview of homophilic and heterophilic *trans*- and *cis*-interactions between TAMPs and claudins in the membranes of bicellular contacts of transfected HEK-293 cells

Protein	Occl	Tric	Md3	Cld1	Cld2	Cld3	Cld4	Cld5	Cld11	Cld12
Standardized enrichment (%)										
Occl	17			29				30		
Tric		0		97				12		
Md3			1	2				0		
Cld1				100		69*		103*		
Cld3						44*		16*		
Cld5								55*		
Cld11									41	
Cld12										5*
Standardized FRET value (%)										
Occl	53	0	43	51	14	5	17	0	0	
Tric		21	45	79	0	18	22	16	0	
Md3			46	46	0	47	23	18	0	
Cld1						78*		70*		
Cld2						9*				
Cld3						67*		48*		
Cld5								100		

Data are related to the homologous *cis*-interaction of Cld5 and to the homologous *trans*-interaction of Cld1, respectively.
*Data determined under comparable experimental conditions by Piontek and colleagues (Piontek et al., 2011) as used in the study presented.

and the incorporation in the TJ network, Occl and Md3 are incorporated with Cld1, Md3 additionally with Cld3, at the bicellular contacts. Furthermore, the mobility of Occl is drastically decreased by Cld1. Md3 is indirectly attracted to bicellular contacts by Occl along which itself is immobilized by Cld1. Nevertheless, the associations of Md3 remain more flexible reflected by the lack of homophilic co-enrichment of Md3 at cell–cell contacts and the lack of changes in the plasma membrane mobility after coexpression with Cld1. However, all members of the TAMP family have the potential to organize the Cld-based TJ network in a specific manner. The general relevance of Tric at bicellular contacts, in the presence of Occl is unclear. But, at tricellular contacts a strong influence of Tric on the TJ structure is expected as demonstrated by functional analyses of tricellular contacts (Krug et al., 2009). In conclusion, our study enlightens the dynamic assembly of TJ networks and clearly indicates the role of the TAMP family as major modulators of the Cld-based TJ strands.

In general, the homophilic and heterophilic associations between most of the classic Clds are stronger than those of the TAMPs (Table 1). Therefore, Clds are able to form the central backbone of the TJ strands. Interactions of the Clds with TAMPs determine the behavior of the TAMPs like membrane mobility, binding properties and localization. On the other hand, TAMPs improve the TJ strand network to obtain the typical physiological morphology of Cld TJ strands.

Materials and Methods

Cell culture, transfection and immunocytochemistry

HEK-293 (Piontek et al., 2011), MDCK-II (Piehl et al., 2010) and Caco-2 (Winkler et al., 2009) cells were cultured in Dulbecco's modified Eagle's medium (DMEM, Invitrogen, Darmstadt, Germany) containing 10% (v/v) fetal calf serum, 100 units/ml penicillin, 100 µg/ml streptomycin, and 1% L-alanyl-L-glutamine (Invitrogen, Darmstadt, Germany). Transient mono-, co- and triple-transfections were performed using polyethylenimin (PEI) according to the supplier's recommendations (Polysciences, Eppelheim, Germany). Polyclonal antibodies against ZO-1, Occl, Tric and Cld1 were purchased from Zymed (Wien, Austria), Alexa-Fluor-488- and Cy3-labeled antibodies were from Invitrogen (Darmstadt, Germany). Rabbit anti-Md3 antibody was kindly provided by Jerry Turner/Chicago, USA.

MDCK-II or Caco-2 cells (7×10^5 cells per 1.8 cm^2) were seeded on glass coverslips coated with poly-L-lysine (Sigma, Hamburg, Germany). After 48 h, cells were washed with phosphate buffered saline (PBS) with Mg^{2+}/Ca^{2+}, fixed with acetone (5 min, 4℃), ethanol (1 min, 4℃) and washed again with PBS (Mg^{2+}/Ca^{2+}). Non-specific binding was blocked with 1% (v/v) BSA in PBS (Mg^{2+}/Ca^{2+}) for 1 h before the primary antibodies were added for 1 h at room temperature. After five washing steps with PBS (Mg^{2+}/Ca^{2+}), the secondary antibodies, and DAPI (4′,6-diamidin-2-phenylindol; Invitrogen, Darmstadt, Germany) were added for 30 min at room temperature. Cells were washed again with PBS (Mg^{2+}/Ca^{2+}), and coverslips mounted on the object plate using Immu-Mount (Thermo Scientific, Ulm, Germany) (Piehl et al., 2010).

For live-cell imaging, transfected cells were transferred to 1 ml Hanks' balanced salt solution (HBSS; Invitrogen, Darmstadt, Germany) pH 7.5. The plasma membrane was visualized with Trypan Blue (final concentration: 0.05%; Sigma, Hamburg, Germany). Cells were examined with a LSM (laser scanning microscope) 510 META system, using an Axiovert 135 microscope equipped with a Plan-Neofluar 100×/1.3 NA objective (Zeiss, Jena, Germany). CFP and YFP were excited at 458 and 514 nm and detected from 463–495 and 527–634 nm, respectively. Trypan Blue was analyzed with 543 nm and 590 nm. For DAPI, excitation was 364 nm and emission 385 to 470 nm. The thickness of optical sections was 0.9 µm.

Cloning of proteins and preparation of expression constructs

Expression vectors for Clds were based on pECFP-N1/pEYFP-N1 or pcDNA-NCFP/-NYFP, for Occl and Md3 (the latter, kind gift from Maria Balda, University College, London) on pECFP-C1/pEYFP-C1 (Clontech, Mountain View, USA) (Piontek et al., 2011). Plasmids for CFP-Tric/YFP-Tric were described previously (Westphal et al., 2010). Cld constructs, corticotropin releasing factor receptor-1–YFP and –CFP were used as described previously (Piontek et al., 2011). Plasmids encoding CFP– and YFP–Occl were generated by PCR amplification of the cDNA with primers introducing the digestion sites for *Sac*I (Fermentas, St. Leon-Rot, Germany) and *Kpn*I (Fermentas), followed by ligation into the pECFP-C1 or pEYFP-C1 vector, respectively. Similarly, plasmids encoding CFP– and YFP–Md3 were generated with digestion sites *Hin*dIII and *Bam*HI (Fermentas). FLAG–Cld1 was kindly provided by S. Müller (Berlin). The position of CFP, YFP and FLAG before or after the protein name describes N- or C-terminal position. The origin of the proteins was human except Cld3, and -5 which were murine.

Transcellular cell scan of fluorescence

To quantify *trans*-interactions of TJ proteins, between the surface of two opposing cells, transcellular cell scans were executed (Piontek et al., 2008). We determined the fluorescence intensity of YFP or CFP, that colocalizes with the fluorescence of the membrane marker Trypan Blue in the intensity profiles along a cell scan. Thus, the intensity ratio and enrichment factor, respectively, at a cell–cell contact was calculated. That means, half the fluorescence intensity of a YFP- or CFP-tagged protein at the contacts between two transfected cells was divided by the fluorescence of YFP or CFP at contacts between an expressing and a non-expressing cell. In case of a *trans*-interaction, the ratio/factor was >1. As positive control, Cld1-transfected cells were used showing strong homophilic *trans*-interaction, corticotropin releasing factor receptor-1 was taken as negative control which does not *trans*-interact (Piontek et al., 2008).

Fluorescence resonance energy transfer

For analysis of the *cis*-interaction between TJ proteins along the cell membrane of one cell, HEK-293 cells growing on coverslips or chambered coverglasses were co- or

triple-transfected with the differently fluorescence labeled Cld or TAMP constructs. After 3 days, cells were transferred into HBSS pH 7.5 or 4-(2-hydroxyethyl)-1-piperazineethanesulfonic acid pH 7.5 buffer and analyzed by LSM. For FRET, acceptor photobleaching was applied as described earlier in cell–cell contacts (supplementary material Fig. S1) (Blasig et al., 2006) or intracellularly (Piontek et al., 2011). The pairs Cld5–CFP/corticotropin releasing factor receptor-1–YFP and Cld1–YFP/corticotropin releasing factor receptor-1–CFP were chosen as negative controls, as they represent transmembrane proteins which colocalize but do not interact with each other (Piontek et al., 2011). Cld5–CFP/Cld5–YFP served as positive control, known to *cis*-interact with each other (Blasig et al., 2006). For the measurements, always areas with similar CFP and YFP fluorescence intensities were analyzed.

Fluorescence recovery after photobleaching

Transfected HEK-293 cells were grown as confluent monolayers on 10 cm^2 glass coverslips (Menzel, Braunschweig, Germany) and imaged in HBSS. Fluorescence bleaching and imaging were performed using a LSM 510 META UV system, using an Axiovert 135 microscope equipped with a PlanNeofluar 100×/1.3 NA oil immersion objective (Carl Zeiss, Jena, Germany). Images were collected every second until steady-state fluorescence was reached. Raw data were aligned and mean fluorescence of background, whole-cell, and bleached bicellular TJ regions were quantified over time using Microsoft Excel 2007. Data correction and mobile fraction were determined as described (Yguerabide et al., 1982) using Microsoft Excel 2007. The measurements were always performed in cell–cell contacts with similar YFP fluorescence intensities.

siRNA knockdown

Caco-2 cells were plated on coverslips (1.8 cm^2) and transfected as described above. One hour prior to the transfection, Caco-2 standard medium was replaced by 400 µl of transfection medium. For each transfection batch, 1 µl Lipofectamine™ 2000 according to the supplier's recommendations (Invitrogen, Darmstadt, Germany) was incubated for 5 min in 50 µl Opti-modified Eagle's medium (Opti-MEM) at room temperature. Additionally, 1 µg of Cld1-siRNA (15 µg/µl) were added to 50 µl Opti-MEM; a scrambled siRNA of Cld1 served as the control (Quiagen, Darmstadt, Germany). Both batches were mixed with each other, 20 min incubated at room temperature and finally trickled at the cells. siRNA/Lipofectamine™ 2000 solution was replaced by Caco-2 standard medium after 6 h. Immunostaining of the cells for Cld1, Tric, and ZO-1 was performed after 48 h of incubation at 37℃ with 10% CO_2. The target DNA sequence of Cld1 was 5′-GAGGATTTACTCCTATGCCGG-3′, and siRNA (5′-GGAUUUACUCCUAUGCCGGtt-3′, 5′-CCGGCAUAGGAGUAAAUCCtc-3′) were used as annealed oligonucleotides.

Freeze-fracture electron microscopy

HEK-293 cells were transfected with Cld and/or TAMP constructs. Three days later, the cells were washed with PBS, fixed with 2.5% glutaraldehyde (electron microscopy grade; Sigma, Hamburg, Germany) in PBS for 2 h, washed and processed for freeze-fracture electron microscopy as reported (Wolburg et al., 2003).

Proximity ligation assay

MDCK-II cells were fixed and incubated (as described above under immunocytochemistry) using rabbit anti-Cld1, mouse anti-Occl and mouse anti-glyceraldehyde-3-phosphate (Serotec, Dusseldorf, Germany) antibodies. Subsequent Duolink® II Proximity Ligation Assay (PLA) was performed according to the manual provided by OLINK Bioscience (Uppsala, Sweden) using PLA probe anti-mouse plus, PLA probe anti-rabbit minus and detection reagent far red. PLA signals were detected by confocal microscopy.

Statistics

Unless stated otherwise, results are shown as means ± s.e.m. Statistical analyses were performed by one-way analysis of variance and followed by an unpaired Student's *t*-test.

Acknowledgements

We thank J. Turner, Chicago, USA, for anti-Md3 antibody, M. Balda, London, UK, for Md3 cDNA, R. Knittel for help with freeze-fracturing and Bianca Hube for the excellent technical assistance.

Funding

This work was supported by the Deutsche Forschungsgemeinschaft [grant numbers BL 308/7-4 to I.E.B.; and FOR721/2 TP5 and TP7 to I.E.B. and D.G., respectively].

Supplementary material available online at
http://jcs.biologists.org/lookup/suppl/doi:10.1242/jcs.114306/-/DC1

References

Amasheh, S., Meiri, N., Gitter, A. H., Schöneberg, T., Mankertz, J., Schulzke, J. D. and Fromm, M. (2002). Claudin-2 expression induces cation-selective channels in tight junctions of epithelial cells. *J. Cell Sci.* **115**, 4969-4976.

Andreeva, A. Y., Piontek, J., Blasig, I. E. and Utepbergenov, D. I. (2006). Assembly of tight junction is regulated by the antagonism of conventional and novel protein kinase C isoforms. *Int. J. Biochem. Cell Biol.* **38**, 222-233.

Angelow, S., Ahlstrom, R. and Yu, A. S. L. (2008). Biology of claudins. *Am. J. Physiol. Renal Physiol.* **295**, F867-F876.

Bal, M. S., Castro, V., Piontek, J., Rueckert, C., Walter, J. K., Shymanets, A., Kurig, B., Haase, H., Nürnberg, B. and Blasig, I. E. (2012). The hinge region of the scaffolding protein of cell contacts, zonula occludens protein 1, regulates interacting with various signaling proteins. *J. Cell. Biochem.* **113**, 934-945.

Basuroy, S., Seth, A., Elias, B., Naren, A. P. and Rao, R. (2006). MAPK interacts with occludin and mediates EGF-induced prevention of tight junction disruption by hydrogen peroxide. *Biochem. J.* **393**, 69-77.

Blasig, I. E., Winkler, L., Lassowski, B., Mueller, S. L., Zuleger, N., Krause, E., Krause, G., Gast, K., Kolbe, M. and Piontek, J. (2006). On the self-association potential of transmembrane tight junction proteins. *Cell. Mol. Life Sci.* **63**, 505-514.

Blasig, I. E., Bellmann, C., Cording, J., del Vecchio, G., Zwanziger, D., Huber, O. and Haseloff, R. F. (2011). Occludin protein family: oxidative stress and reducing conditions. *Antioxid. Redox Signal.* **15**, 1195-1219.

Chen, Y. H., Lu, Q., Goodenough, D. A. and Jeansonne, B. (2002). Nonreceptor tyrosine kinase c-Yes interacts with occludin during tight junction formation in canine kidney epithelial cells. *Mol. Biol. Cell* **13**, 1227-1237.

Dörfel, M. J. and Huber, O. (2012). Modulation of tight junction structure and function by kinases and phosphatases targeting occludin. *J. Biomed Biotechnol.* **2012**, DOI: 10.1155/2012/807356.

Dörfel, M. J., Westphal, J. K. and Huber, O. (2009). Differential phosphorylation of occludin and tricellulin by CK2 and CK1. *Ann. N. Y. Acad. Sci.* **1165**, 69-73.

Furuse, M., Hirase, T., Itoh, M., Nagafuchi, A., Yonemura, S., Tsukita, S. and Tsukita, S. (1993). Occludin: a novel integral membrane protein localizing at tight junctions. *J. Cell Biol.* **123**, 1777-1788.

Furuse, M., Fujita, K., Hiiragi, T., Fujimoto, K. and Tsukita, S. (1998). Claudin-1 and -2: novel integral membrane proteins localizing at tight junctions with no sequence similarity to occludin. *J. Cell Biol.* **141**, 1539-1550.

Furuse, M., Sasaki, H. and Tsukita, S. (1999). Manner of interaction of heterogeneous claudin species within and between tight junction strands. *J. Cell Biol.* **147**, 891-903.

Harris, H. J., Davis, C., Mullins, J. G. L., Hu, K., Goodall, M., Farquhar, M. J., Mee, C. J., McCaffrey, K., Young, S., Drummer, H. et al. (2010). Claudin association with CD81 defines hepatitis C virus entry. *J. Biol. Chem.* **285**, 21092-21102.

Ikenouchi, J., Furuse, M., Furuse, K., Sasaki, H., Tsukita, S. and Tsukita, S. (2005). Tricellulin constitutes a novel barrier at tricellular contacts of epithelial cells. *J. Cell Biol.* **171**, 939-945.

Ikenouchi, J., Sasaki, H., Tsukita, S., Furuse, M. and Tsukita, S. (2008). Loss of occludin affects tricellular localization of tricellulin. *Mol. Biol. Cell* **19**, 4687-4693.

Itoh, M., Furuse, M., Morita, K., Kubota, K., Saitou, M. and Tsukita, S. (1999). Direct binding of three tight junction-associated MAGUKs, ZO-1, ZO-2, and ZO-3, with the COOH termini of claudins. *J. Cell Biol.* **147**, 1351-1363.

Kale, G., Naren, A. P., Sheth, P. and Rao, R. K. (2003). Tyrosine phosphorylation of occludin attenuates its interactions with ZO-1, ZO-2, and ZO-3. *Biochem. Biophys. Res. Commun.* **302**, 324-329.

Krause, G., Winkler, L., Mueller, S. L., Haseloff, R. F., Piontek, J. and Blasig, I. E. (2008). Structure and function of claudins. *Biochim. Biophys. Acta* **1778**, 631-645.

Krug, S. M., Amasheh, S., Richter, J. F., Milatz, S., Günzel, D., Westphal, J. K., Huber, O., Schulzke, J. D. and Fromm, M. (2009). Tricellulin forms a barrier to macromolecules in tricellular tight junctions without affecting ion permeability. *Mol. Biol. Cell* **20**, 3713-3724.

Marchiando, A. M., Shen, L., Graham, W. V., Weber, C. R., Schwarz, B. T., Austin, J. R., 2nd, Raleigh, D. R., Guan, Y. F., Watson, A. J. M., Montrose, M. H. et al. (2010). Caveolin-1-dependent occludin endocytosis is required for TNF-induced tight junction regulation in vivo. *J. Cell Biol.* **189**, 111-126.

Masuda, S., Oda, Y., Sasaki, H., Ikenouchi, J., Higashi, T., Akashi, M., Nishi, E. and Furuse, M. (2011). LSR defines cell corners for tricellular tight junction formation in epithelial cells. *J. Cell Sci.* **124**, 548-555.

Mineta, K., Yamamoto, Y., Yamazaki, Y., Tanaka, H., Tada, Y., Saito, K., Tamura, A., Igarashi, M., Endo, T., Takeuchi, K. et al. (2011). Predicted expansion of the claudin multigene family. *FEBS Lett.* **585**, 606-612.

Müller, S. L., Portwich, M., Schmidt, A., Utepbergenov, D. I., Huber, O., Blasig, I. E. and Krause, G. (2005). The tight junction protein occludin and the adherens junction protein alpha-catenin share a common interaction mechanism with ZO-1. *J. Biol. Chem.* **280**, 3747-3756.

Nitta, T., Hata, M., Gotoh, S., Seo, Y., Sasaki, H., Hashimoto, N., Furuse, M. and Tsukita, S. (2003). Size-selective loosening of the blood-brain barrier in claudin-5-deficient mice. *J. Cell Biol.* **161**, 653-660.

Piehl, C., Piontek, J., Cording, J., Wolburg, H. and Blasig, I. E. (2010). Participation of the second extracellular loop of claudin-5 in paracellular tightening against ions, small and large molecules. *Cell. Mol. Life Sci.* **67**, 2131-2140.

Piontek, J., Winkler, L., Wolburg, H., Müller, S. L., Zuleger, N., Piehl, C., Wiesner, B., Krause, G. and Blasig, I. E. (2008). Formation of tight junction: determinants of homophilic interaction between classic claudins. *FASEB J.* **22**, 146-158.

Piontek, J., Fritzsche, S., Cording, J., Richter, S., Hartwig, J., Walter, M., Yu, D., Turner, J. R., Gehring, C., Rahn, H. P. et al. (2011). Elucidating the principles of the molecular organization of heteropolymeric tight junction strands. *Cell. Mol. Life Sci.* **68**, 3903-3918.

Raleigh, D. R., Marchiando, A. M., Zhang, Y., Shen, L., Sasaki, H., Wang, Y. M., Long, M. Y. and Turner, J. R. (2010). Tight junction-associated MARVEL proteins marveld3, tricellulin, and occludin have distinct but overlapping functions. *Mol. Biol. Cell* **21**, 1200-1213.

Raleigh, D. R., Boe, D. M., Yu, D., Weber, C. R., Marchiando, A. M., Bradford, E. M., Wang, Y. M., Wu, L. C., Schneeberger, E. E., Shen, L. et al. (2011). Occludin S408 phosphorylation regulates tight junction protein interactions and barrier function. *J. Cell Biol.* **193**, 565-582.

Riazuddin, S., Ahmed, Z. M., Fanning, A. S., Lagziel, A., Kitajiri, S., Ramzan, K., Khan, S. N., Chattaraj, P., Friedman, P. L., Anderson, J. M. et al. (2006). Tricellulin is a tight-junction protein necessary for hearing. *Am. J. Hum. Genet.* **79**, 1040-1051.

Saitou, M., Furuse, M., Sasaki, H., Schulzke, J. D., Fromm, M., Takano, H., Noda, T. and Tsukita, S. (2000). Complex phenotype of mice lacking occludin, a component of tight junction strands. *Mol. Biol. Cell* **11**, 4131-4142.

Schulzke, J. D., Gitter, A. H., Mankertz, J., Spiegel, S., Seidler, U., Amasheh, S., Saitou, M., Tsukita, S. and Fromm, M. (2005). Epithelial transport and barrier function in occludin-deficient mice. *Biochim. Biophys. Acta* **1669**, 34-42.

Sekar, R. B. and Periasamy, A. (2003). Fluorescence resonance energy transfer (FRET) microscopy imaging of live cell protein localizations. *J. Cell Biol.* **160**, 629-633.

Shen, L., Weber, C. R. and Turner, J. R. (2008). The tight junction protein complex undergoes rapid and continuous molecular remodeling at steady state. *J. Cell Biol.* **181**, 683-695.

Steed, E., Rodrigues, N. T. L., Balda, M. S. and Matter, K. (2009). Identification of MarvelD3 as a tight junction-associated transmembrane protein of the occludin family. *BMC Cell Biol.* **10**, doi:10.1186/1471-2121-10-95.

Walter, J. K., Rueckert, C., Voss, M., Mueller, S. L., Piontek, J., Gast, K. and Blasig, I. E. (2009). The oligomerization of the coiled coil-domain of occluddin is redox sensitive. In *Molecular Structure and Function of the Tight Junction: From Basic Mechanisms to Clinical Manifestations*, vol. 1165 (ed. M. Fromm and J. D. Schulzke), pp. 19-27. Boston, MA: Blackwell Publishing.

Westphal, J. K., Dörfel, M. J., Krug, S. M., Cording, J. D., Piontek, J., Blasig, I. E., Tauber, R., Fromm, M. and Huber, O. (2010). Tricellulin forms homomeric and heteromeric tight junctional complexes. *Cell. Mol. Life Sci.* **67**, 2057-2068.

Winkler, L., Gehring, C., Wenzel, A., Müller, S. L., Piehl, C., Krause, G., Blasig, I. E. and Piontek, J. (2009). Molecular determinants of the interaction between Clostridium perfringens enterotoxin fragments and claudin-3. *J. Biol. Chem.* **284**, 18863-18872.

Wolburg, H., Liebner, S. and Lippoldt, A. (2003). Freeze-fracture studies of cerebral endothelial tight junctions. *Methods Mol. Med.* **89**, 51-66.

Yguerabide, J., Schmidt, J. A. and Yguerabide, E. E. (1982). Lateral mobility in membranes as detected by fluorescence recovery after photobleaching. *Biophys. J.* **40**, 69-75.